Effect of Aging on the Mechanical Properties of Poly(3-hydroxybutyrate-*co*-3-hydroxyhexanoate)

Hexig Alata,[†] Taizo Aoyama,[‡] and Yoshio Inoue*,[†]

Department of Biomolecular Engineering, Tokyo Institute of Technology, Nagatsuta 4259-B55, Midori-ku, Yokohama 226-8501, Japan, and Research & Development Group, Performance Polymer Division, Kaneka Corporation, 5-1-1, Torikai-Nishi, Settsu, Osaka 566-0072, Japan

Received February 16, 2007; Revised Manuscript Received April 26, 2007

ABSTRACT: The effect of aging on the mechanical properties was investigated for a series of bacterial copolyester poly(3-hydroxybutyrate-*co*-3-hydroxyhexanoate) [P(3HB-*co*-3HH)] with 3HH molar fraction ranging from 5 to 18 mol %. The mechanism behind the aging phenomenon was studied by using gel permeation chromatography (GPC), differential scanning calorimetry (DSC), wide-angle X-ray diffraction (WAXD), and small-angle X-ray scattering (SAXS) in parallel to the tensile testing. It was found that the high initial crystallinity and the narrower amorphous region in the P(3HB-*co*-3HH) films are the key factors that cause the secondary crystallization in the aging process to embrittle the films of copolymers with 3HH fraction lower than 10 mol %. For the copolymers with 3HH fractions higher than 10 mol %, because of the intrinsically lower crystallinity and thicker amorphous region, the secondary crystallization cannot affect the mechanical properties significantly.

Introduction

With the increasing concern of human society to environmental and energy problems, the family of microbially synthesized polymers poly(hydroxyalkanoates) (PHAs) have been attracting more and more attention in both academic and industrial fields due to their complete biodegradability and the renewable carbon resources used to produce them.[1,2] Poly(3-hydroxybutyrate)(PHB) is the first found one of the PHA family[3] and can be produced by a wide range of bacteria, but it is rigid and stiff because of the high crystallinity and big-size spherulites.[4−6] PHB is also thermally unstable during the conventional melt processing due to the high melting temperature.[7] To improve the overall physical properties of PHB, PHAs containing over 125 types of monomers have been synthesized in different microorganisms.[8] The copolymers show a wide range of physical properties depending on the chemical structure of the comonomer units as well as the comonomer composition.

Poly(3-hydroxybutyrate-*co*-3-hydroxyvelerate) [P(3HB-*co*-3HV)] is the first commercialized bacterial copolyester under the trade name of Biopol.[9] But P(3HB-*co*-3HV) shows an unusual phenomenon of isodimorphism, i.e., due to the similarity in the shape and size between the 3HB and 3HV units, they can incorporate into the crystal lattice of each other, and cause high crystallinity over the entire range of comonomer composition.[10−12] Due to the isodimorphism, the properties of P(3HB-*co*-3HV) are not significantly improved in comparison to those of P(3HB) homopolymer. The 3-hydroxyhexanoate unit with medium length side groups was incorporated into the molecular chain of PHB to attain more desirable properties.[13−15] It was reported that the crystallinity of poly(3-hydroxybutyrate-*co*-3-hydroxyhexanoate)s [P(3HB-*co*-3HH)s] was decreased from 60% to 26%, and the elongation to break increased from 5% to 850% with the increase of 3HH molar fraction from 0 to 17 mol %.[14] Furthermore, the melting temperature of P(3HB-*co*-3HH) decreases steeply with the increase of 3HH molar fraction.[14−16]

P(3HB) and P(3HB-*co*-3HV) are known to undergo secondary crystallization, which reduces the number of polymer chains in the amorphous phase, resulting in a detrimental embrittlement of the materials.[17−19] It was believed that P(3HB-*co*-3HH) copolymers containing longer side chain 3HH comonomers that do not cocrystallize would exhibit minimal secondary crystallization and, hence, no significant aging effect. However, it was reported that the P(3HB-*co*-3HH) copolymers with 3HH molar fraction ranging from 2.5 to 8.1 mol % exhibited the typical signs of polymer aging phenomenon, the elongation was reduced and the strength was increased after 11 days of room-temperature aging.[15] Because the aging phenomenon is concerned with the practical applicability of polymers, it is of great importance to carry out a systematic study on it. In this work, the aging phenomenon of P(3HB-*co*-3HH) copolymers with wider 3HH molar fraction ranging from 5 to 18 mol % was studied, and efforts also have been contributed to investigate the mechanism behind the aging phenomenon of this copolymer.

Experimental Section

Materials and Sample Preparation. A series of bacterial P(3HB-*co*-3HH) samples with 3HH molar fractions 5, 7, 10, 12, and 18 mol %, respectively, were kindly supplied by Kaneka Corporation, Osaka, Japan. The P(3HB-*co*-3HH) films were prepared by solution casting from their chloroform solutions using Teflon Petri dishes as casting surfaces, allowing the solvent to evaporate at room temperature for 1 day and then drying at 40 °C in vacuum for 1 day to remove the residual solvent. After that the first day's measurements were performed, and the remained films were aged in vacuum oven at room temperature.

Tensile Test. Tensile properties were measured at room temperature using an EZ test machine (Shimadzu Corp., Tokyo, Japan). The gauge length and crosshead speed were 22.25 and 20 mm/min, respectively. The sample thickness was ca. 0.1 mm. At least five samples were tested and the average was used.

Gel Permeation Chromatography (GPC). Variation of the molecular weight distribution was investigated by gel permeation chromatography at 25 °C, using a Tosoh HLC-8020 system with TSK GEL G2000Hxl and GMHxl columns. The concentration of

* E-mail: inoue.y.af@m.titech.ac.jp.
[†] Department of Biomolecular Engineering, Tokyo Institute of Technology.
[‡] Research & Development Group, Performance Polymer Division, Kaneka Corporation.

10.1021/ma070418i CCC: $37.00
Published on Web 06/01/2007

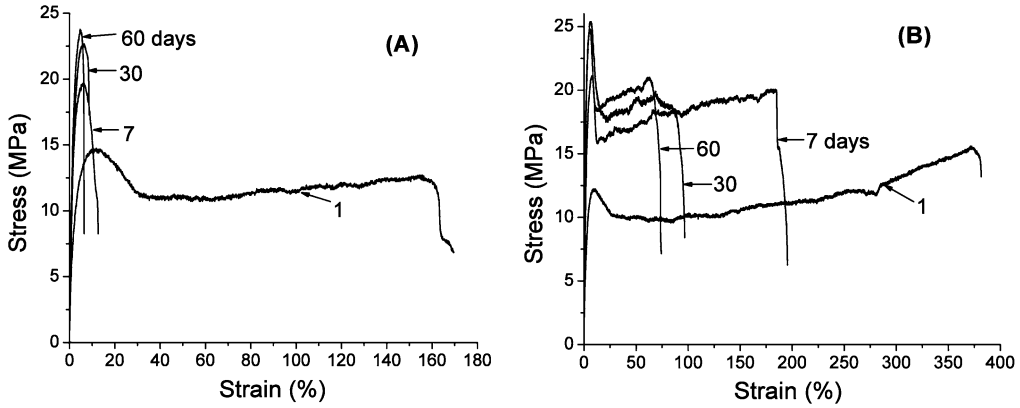

Figure 1. Stress−strain curves of (A) P(3HB-*co*-5 mol % 3HH), and (B) P(3HB-*co*-7 mol % 3HH) films after different periods of aging. The aging times, in days, are indicated in the curves.

Table 1. Effect of Aging on the Material Properties of P(3HB-*co*-3HH) Samples[a]

sample	aging period (day)	tensile strength (Mpa)	elongation to break (%)	crystallinity (%)	heat of fusion (J/g)	T_g (°C)
P(3HB-*co*-5%3HH)	1	12.8	163.6	41.6 ± 5	69.2	−5.3
	7	19.6	12.7	44.5 ± 5	71.6	−4.3
	30	22.4	8.6	47.7 ± 5	72.5	1.2
	60	23.6	6.5	47.9 ± 5		
P(3HB-*co*-7%3HH)	1	15.3	381.4	39.9 ± 5	66.7	−5.0
	7	19.7	195.2	41.2 ± 5	69.1	−3.4
	30	19.2	96.8	45.8 ± 5	71.5	−1.4
	60	20.2	73.4	46.3 ± 5	72.9	N.D.
P(3HB-*co*-10%3HH)	1	14.9	469.9	30.1 ± 5	58.2	−6.4
	7	14.7	456.4	34.7 ± 5	61.4	−5.9
	30	17.2	451.9	35.7 ± 5	61.8	−6.2
	60	15.1	387.8	35.9 ± 5	66.1	−5.8
P(3HB-co-12%3HH)	1	20.1	579.5	30.7 ± 5	52.4	−6.9
	7	21.9	573.3	32.7 ± 5	54.1	−6.2
	30	21.9	561.3	36.8 ± 5	57.2	−6.2
	60	22.9	549.1	37.7 ± 5	57.7	−6.3
P(3HB-co-18%3HH)	1	12.7	660.5	25.1 ± 5	45.7	−8.1
	7	13.4	650.4	27.4 ± 5	48.6	−8.0
	30	14.7	650.6	31.7 ± 5	52.7	−8.0
	60	13.9	538.2	29.3 ± 5	54.2	−7.9

[a] N.D.: not detected.

the samples in chloroform is 1 mg/mL, and the injection volume is 100 μL. Chloroform was used as the eluent at a flow rate of 1.0 mL/min. The polystyrene samples with low polydispersity were used to make a calibration curve.

Wide-Angle X-ray Diffraction (WAXD) and Small-Angle X-ray Scattering (SAXS) Measurements. WAXD and SAXS measurements were carried out on a Rigaku RU-200 system using nickel-filtered Cu Kα radiation ($\lambda = 0.154$ nm) operated at 40 kV and 200 mA. The WAXD patterns were recorded in the 2θ range of 5−60° at a scan speed of 1.0 °/min. The percentage of crystallinity was calculated from diffracted intensity data according to Vonk's method.[20] SAXS profiles were recorded in the 2θ range of 0.1−3.4°. Each step increased 2θ by 0.004°, and X-ray was collected for 20 s at each step.

Differential Scanning Calorimetry (DSC). DSC measurements were carried out on a Seiko DSC-220 assembled with SSC-580 thermal controller. An 8−10 mg sample was encapsulated in an aluminum pan. The DSC thermogram was recorded from −100 to +190 °C at a heating rate of 10 °C/min. The value of enthalpy of fusion (ΔH) was calculated from the area of the endotherm peak. The glass transition temperature (T_g) was taken as the summit of the peak of the differentiated DSC (DDSC) curves.

Results

Tensile Test. The stress−strain curves of the P(3HB-*co*-5 mol % 3HH) and P(3HB-*co*-7 mol % 3HH) films stored at room temperature for different periods are shown in Figure 1. The effect of aging on the material properties of P(3HB-*co*-3HH) samples was summarized in Table 1. For both P(3HB-*co*-5 mol % 3HH) and P(3HB-*co*-7 mol % 3HH) copolymers, with the increase of aging period, the elongation to break was decreased and the tensile strength was increased. For P(3HB-*co*-5 mol % 3HH), the initial elongation to break and tensile strength were 163.6% and 12.8 MPa, respectively. However, after aged at room temperature for 7 days, the elongation to break decreased to 12.7%, and the tensile strength increased to 19.6 MPa. After aged at room temperature for 30 and 60 days, the elongation to break further decreased to 8.6 and 6.5%, and the tensile strength increased to 22.4 and 23.6 MPa, respectively, reflecting the pronounced effect of aging on the mechanical properties. For P(3HB-*co*-7 mol % 3HH) copolymer, the initial elongation to break and tensile strength were 381.4% and 15.3 MPa, respectively. But after 7, 30, and 60 days of room-temperature aging, the elongation to break dropped to 195.2, 96.8, and 73.4%, respectively, and the tensile strength increased to 19.7, 19.2, and 20.2 MPa, respectively.

The stress−strain curves of the P(3HB-*co*-10 mol % 3HH), P(3HB-*co*-12 mol % 3HH), and P(3HB-*co*-18 mol % 3HH) films stored at room temperature for different periods are shown in Figure 2. For all the three samples, 60 days room-temperature aging did not show any significant effect on the mechanical properties comparing to the copolymers with 3HH molar fractions 5 and 7 mol %. With the increase of aging period, the elongation to break was decreased a little, and the tensile

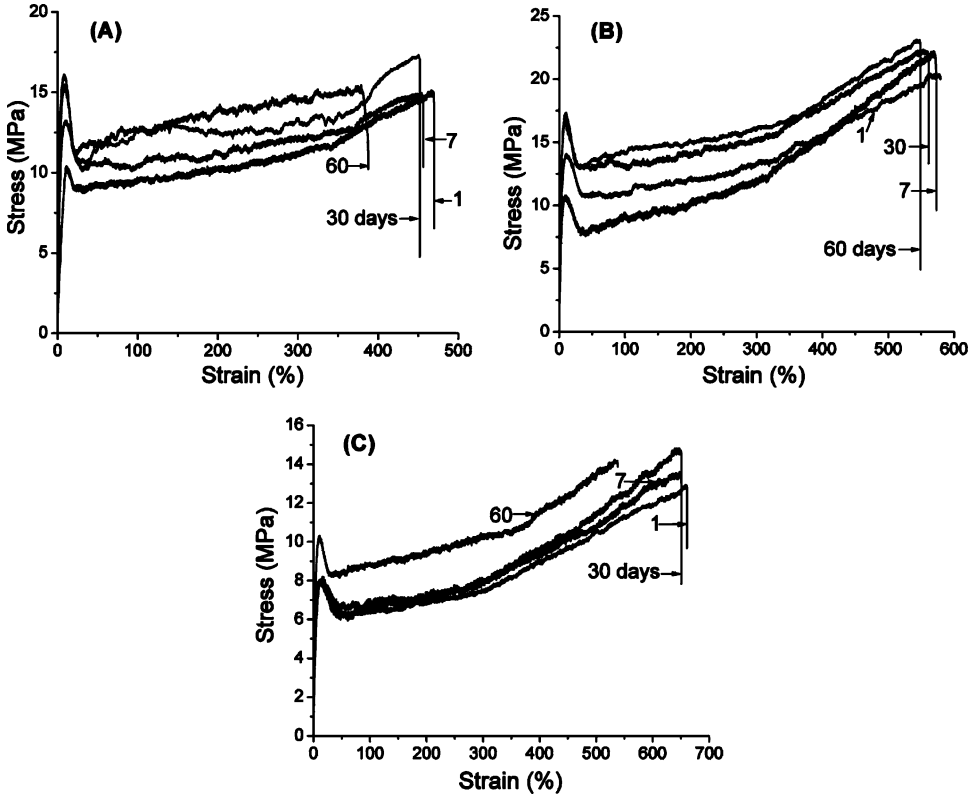

Figure 2. Stress−strain curves of (A) P(3HB-*co*-10 mol % 3HH), (B) P(3HB-*co*-12 mol % 3HH), and (C) P(3HB-*co*-18 mol % 3HH) films after different periods of aging. The aging times, in days, are indicated in the curves.

strength increased slightly. As summarized in Table 1, the initial elongation to break for P(3HB-*co*-3HH) copolymers with 3HH fractions 10, 12, and 18 mol % were 469.9%, 579.5%, and 660.5%, respectively. After being aged at room temperature for 60 days, the final elongations to break for these copolymers were 387.8%, 549.1%, and 538.2%, respectively. The values of percentage reduction of elongation to break for these copolymers were 17.5%, 5.0%, and 18.5%, respectively, while those of the copolymers with 3HH fractions 5 and 7 mol % were 96.0% and 80.8%, respectively. The values of percentage reduction of elongation to break was calculated by the equation $\Delta L\% = (L_i - L_f)/L_i \times 100\%$, where L_i and L_f indicate, respectively, the initial elongation to break and the final elongation to break after being aged at room temperature for 60 days.

GPC Analysis. Because P(3HB-*co*-3HH) is a kind of biodegradable and also hydrolyzable copolyester, there is a possibility that the embrittlement is related to a drop in molecular weight. However, GPC measurements revealed that after 60 days of aging, no noticeable changes in the average molecular weight as well as molecular weight distribution were detected for all the P(3HB-*co*-3HH) copolymers studied in this work, as shown in Figure 3. The number-average molecular weights of the P(3HB-*co*-3HH) copolymers having 3HH molar fractions 5, 7, 10, 12, 18 mol % were 1.68×10^5, 1.24×10^5, 0.92×10^5, 2.17×10^5, and 1.89×10^5, respectively, and the polydispersities were 1.79, 2.24, 1.51, 1.93, and 1.76, respectively.

WAXD and SAXS Measurements. WAXD measurements were performed to study the crystal form and estimate the crystallinity of P(3HB-*co*-3HH) samples. Figure 4A shows the WAXD diffraction patterns of the P(3HB-*co*-3HH) samples in the first day of aging. Only the crystal form of P(3HB) was observed for all the samples with 3HH molar fraction ranging from 5 to 18 mol %. The X-ray crystallinity of P(3HB-*co*-3HH) samples with 3HH molar fractions 5, 7, 10, 12, and 18 mol %

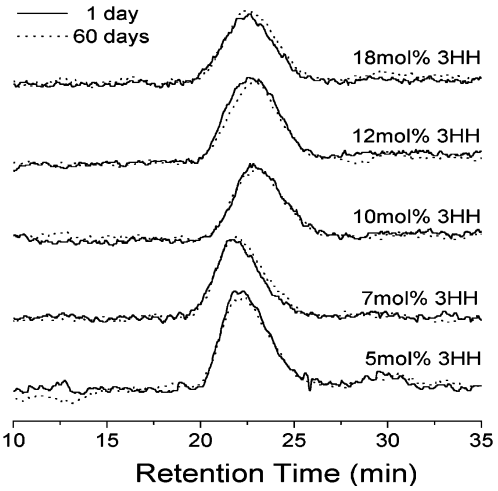

Figure 3. Molecular weight distribution revealed by GPC measurements for the P(3HB-*co*-3HH) initial samples and those after aged at room temperature for 60 days. The 3HH molar fractions in the samples are indicated in the curves.

were 41.6, 39.9, 30.1, 30.7, and 25.1%, respectively. With the increase of aging period, the crystal form did not show any noticeable variation. The crystallinity of the samples as a function of aging time is plotted in Figure 4B. At all the times, the crystallinity of the P(3HB-*co*-3HH) with 3HH molar fraction higher than 10 mol % is much lower than that of the P(3HB-*co*-3HH) with 3HH molar fraction lower than 10 mol %. However, for all the samples, the crystallinity increases with almost the same trend with the increase of aging time up to 30 days, and then it remained almost constant, indicating that the secondary crystallization occurred in all the samples in the first 30 days of room-temperature aging.

The long periods of P(3HB-*co*-3HH) were determined by analysis of the SAXS patterns. Figure 5A shows the SAXS

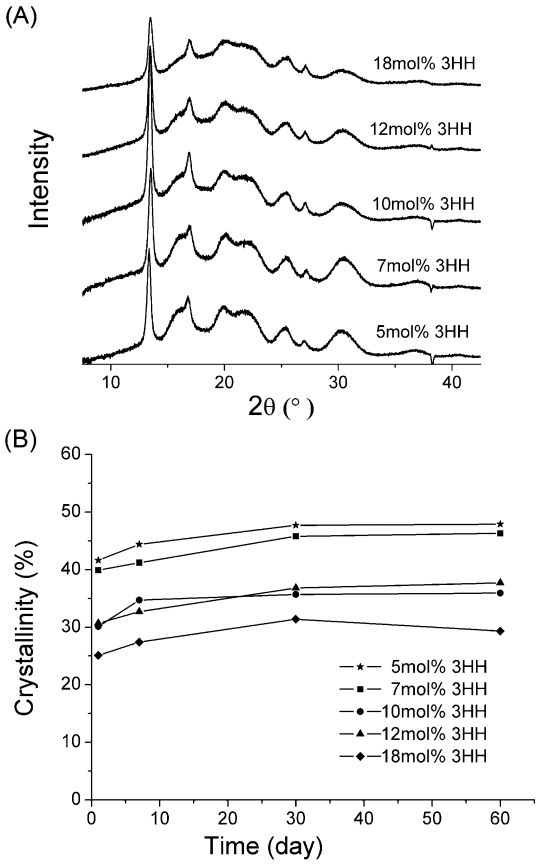

Figure 4. (A) WAXD patterns of P(3HB-*co*-3HH) samples in the first day of aging. (B) The variation of X-ray crystallinity for the P(3HB-*co*-3HH) samples as a function of aging period. The 3HH molar fractions in the samples are indicated in the curves.

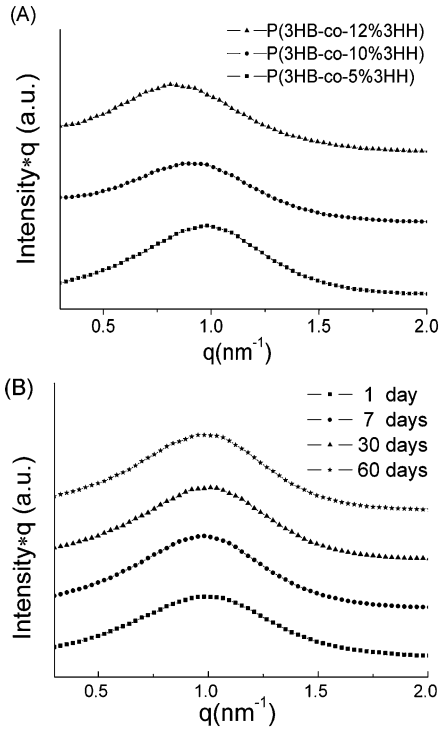

Figure 5. (A) SAXS patterns of P(3HB-*co*-3HH) samples in the first day of aging. (B) SAXS patterns for the P(3HB-*co*-5 mol % 3HH) copolymer after different periods of aging.

patterns for the P(3HB-*co*-5 mol % 3HH), P(3HB-*co*-10 mol % 3HH), and P(3HB-*co*-12 mol % 3HH) films in the first day of aging. The scattering vector magnitude is defined by $q = 4\pi(\sin\theta)/\lambda$, where θ is half the scattering angle and λ is the wavelength of the radiation. The long period (Lp) can be determined by $\mathrm{Lp} = 2\pi/q_{max}$, where q_{max} is the q value at the maximum SAXS intensity. In Figure 5A, for P(3HB-*co*-3HH) with 3HH fractions of 5, 10, and 12 mol %, the q_{max} values were 0.98, 0.89, and 0.79 nm^{-1}, respectively, corresponding to the Lp value of 6.4, 7.1, and 8.0 nm, respectively, indicating that the long period increases with the increase of 3HH fraction. Considering that the incorporation of noncrystallizable 3HH unit into the copolymer leads to the decrease in lamellar thickness,[21] the increase of the long period with the increase of 3HH molar fraction indicate the excess increase of the amorphous thickness than the decrease of lamellar thickness. This result is consistent with that obtained earlier with the aid of two-dimensional Fourier transform infrared spectroscopy (2D FTIR) analysis that the amorphous phase is preferentially formed, whereas the 3HH units are gradually inserted into the random copolymer, and the incorporation of the high fraction of 3HH units into the copolymer chain serves not only as a simple addition of the inert noncrystallizable component but also as an effective means to destroy the crystal structure of this copolymer.[22]

Figure 5B shows the SAXS patterns for the P(3HB-*co*-5 mol % 3HH) films aged at room temperature for different periods. No significant variations can be detected over aging period of 60 days, indicating that the morphology including lamellar thickness and amorphous thickness were not changed with the increase of aging period. This result is the same for all the other samples investigated. The same results were also observed in the early work on PHB. The authors suggested that the constant morphological structure throughout aging specifies secondary crystallization as simple perfection processes in the crystalline−amorphous interface at the expense of the amorphous layer, e.g., the rearrangement of loops in the fold region.[18] For the copolymer P(3HB-*co*-3HH), the crystalline−amorphous interface in this copolymer should be mostly constrained by the noncrystallizable 3HH units. In the previous work of Abe et al.,[21] it was also shown that the isothermal crystallization at elevated temperatures leads to the increase of both the long period and the lamellar thickness in PHB and P(3HB-*co*-3HV), but for P(3HB-*co*-8 mol % 3HH), the lamellar thickness just showed a slight increase that was in the range of experimental error, while the long period increases significantly, indicating that the noncrystallizable 3HH unit restricts the increase of lamellar thickness. Therefore, one possible explanation for the P(3HB-*co*-3HH) copolymer is that the secondary crystallization mainly occurs in the interlamellar amorphous region. However, because the amorphous region is comparatively rich in 3HH units with longer side chains entangled with each other, the crystallization of the 3HB unit only leads to some very tiny crystals which do not lead to any variation in the SAXS patterns but put a tight constraint on the amorphous chains in the interlamellar region.

DSC Measurements. DSC measurements were performed to investigate the variation of glass transition temperature and enthalpy of fusion with the increase of aging period. Figure 6 and Figure 7 show the DSC thermograms of P(3HB-*co*-3HH) copolymers aged at room temperature for different periods. The DDSC curves at glass transition region are also inserted. For all the samples, the melting temperature did not show any significant change with the increase of aging period. As summarized in Table 1 and Figure 8A, the enthalpy of fusion of all the samples increases with the increase of aging period, with the similar trend to the crystallinity variation calculated from WAXD patterns. The DDSC curves of P(3HB-*co*-5 mol

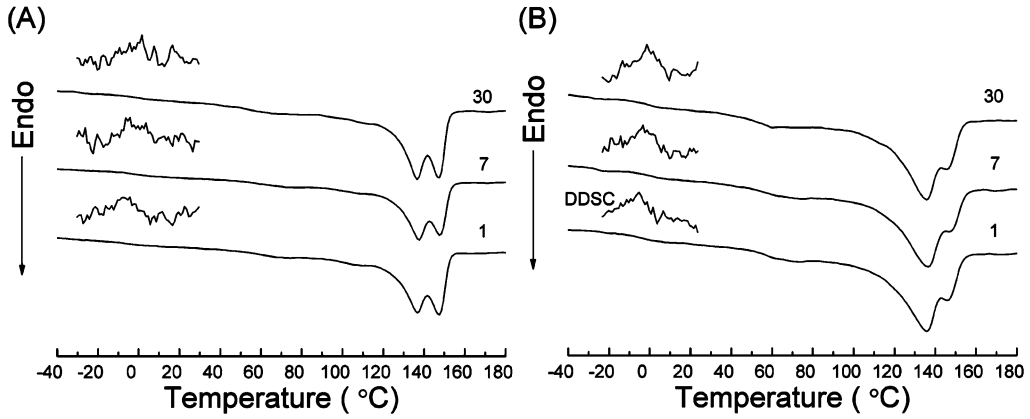

Figure 6. DSC thermograms of (A) P(3HB-*co*-5 mol % 3HH) and (B) P(3HB-*co*-7 mol % 3HH) after different aging period. The DDSC curves at glass transition region are also inserted above the corresponding DSC curves.

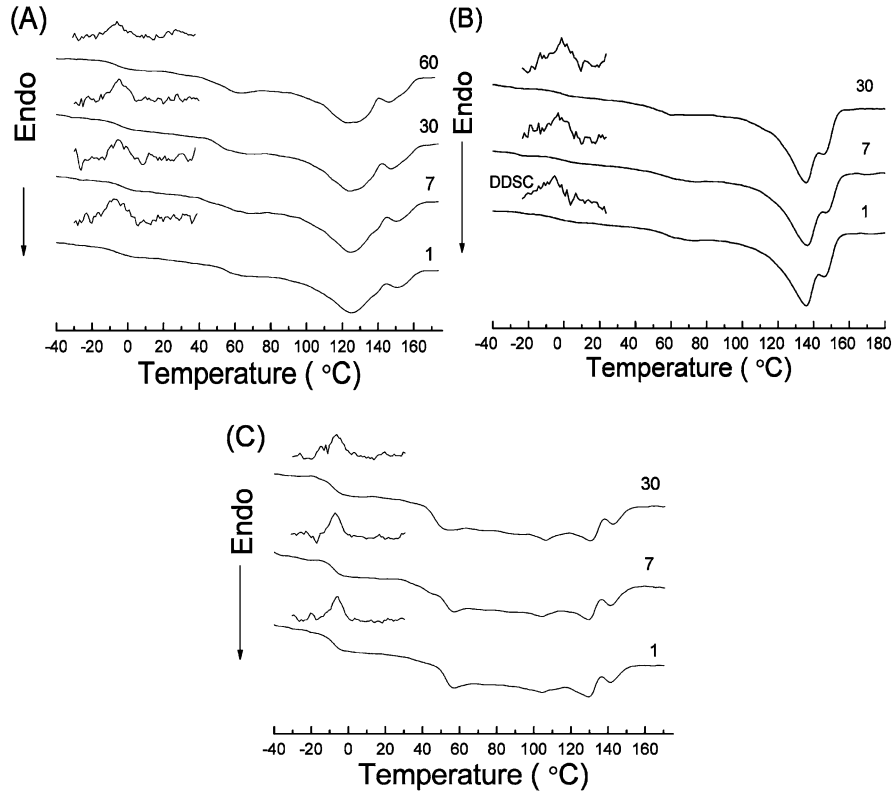

Figure 7. DSC thermograms of (A) P(3HB-*co*-10 mol % 3HH), (B) P(3HB-*co*-12 mol % 3HH), and (C) P(3HB-*co*-18 mol % 3HH) after different aging period. The DDSC curves at glass transition region are also inserted above the corresponding DSC curves.

% 3HH) and P(3HB-*co*-7 mol % 3HH) showed a broad peak at the glass transition region and the peaks shifted to higher temperature side with the increase of aging period. After 60 days aging, the peaks in the DDSC curves at the glass transition region became not detectable in the first heating scan for both copolymers. The DDSC curves of P(3HB-*co*-3HH) copolymer with 3HH fraction of 10, 12, and 18 mol % showed a clear peak at the glass transition region and the peak position showed a little shift to the higher temperature side within the first 7 days aging, and then kept almost constant. The glass transition temperature taken as the peak top of DDSC curves were summarized and compared in Table 1 and Figure 8B. In Figure 8B, it is clearly shown that the glass transition temperature of P(3HB-*co*-3HH) copolymer with 3HH molar fraction 5 and 7 mol % increases much more steeply than that of the P(3HB-*co*-3HH) copolymer with 3HH molar fraction 10, 12, and 18 mol %, indicating that the mobility of the amorphous region of the copolymers with 3HH molar fraction lower than 10 mol % decreases much more significantly than the other copolymers with 3HH fraction higher than 10 mol %, though both the crystallinity calculated from X-ray diffraction patterns and the enthalpy of fusion measured by DSC showed a similar increasing trend for all the copolymers investigated.

Discussion

In the early work,[17,18] de Koning et al. found that the embrittlement of PHB is caused by the secondary crystallization after their initial crystallization from melt. The secondary crystallization seriously constrains the amorphous phase, and hence promotes the embrittlement of PHB. In this work, all the copolymers investigated show the evidence of secondary crystallization, both the crystallinity calculated from X-ray diffraction patterns and the enthalpy of fusion measured by DSC showed a similar increasing trend with the increase of aging period for all the copolymers investigated. However, the embrittlement occurred only in the copolymers with 3HH

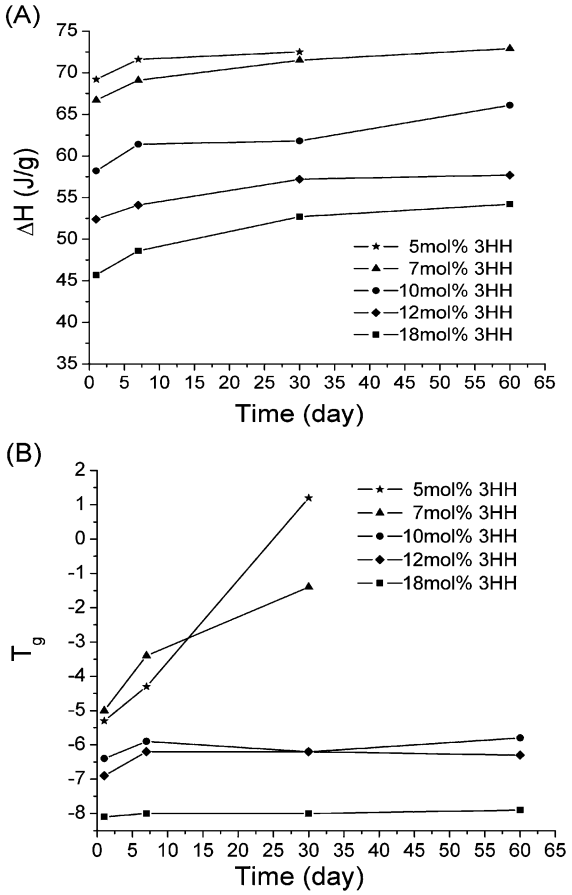

Figure 8. (A) Variation of the enthalpy of fusion for the P(3HB-*co*-3HH) samples as a function of aging period. (B) Variation of the glass transition temperature for the P(3HB-*co*-3HH) samples as a function of aging period. The 3HH molar fractions in the samples are indicated in the curves.

fraction lower than 10 mol %. Comparing the difference among these copolymers investigated, we can notice that the initial crystallinity of the copolymer with 3HH fraction lower than 10 mol % is apparently much higher than that of the copolymer with 3HH fraction higher than 10 mol %, indicating that the constraints imposed on the amorphous chains by the crystals are initially much larger in the copolymer with 3HH fraction lower than 10 mol % than in the copolymer with 3HH fraction higher than 10 mol %, the ability of the amorphous phase to dissipate energy is initially much lower in the copolymer with 3HH fraction lower than 10 mol %. SAXS measurements also revealed that the long period increases with the increase of 3HH fraction, corresponding to the expansion of amorphous region between the individual lamellae. In order to enable plastic deformation, it is essential that the amorphous regions between adjacent crystals allow a certain amount of adjustment to accommodate some rotation of the crystals.[18] The expansion of amorphous region thus implies that the ability of the amorphous region to accommodate such a rotation of the crystals increases with the increase of 3HH fraction. Because the high initial crystallinity and the narrower amorphous region between the individual lamellae, A little increase of crystallinity leads to an even tighter constraint on the amorphous chains between the crystals in the copolymer with 3HH fraction lower than 10 mol %, evidenced by the steep increase of glass transition temperature. As a consequence, the material embrittles. However, for the copolymer with 3HH fraction higher than 10 mol %, though the increasing trend of crystallinity is similar to that of the copolymer with 3HH fraction lower than 10 mol %, the secondary crystallization cannot put such a tight constraint on the amorphous region between the crystals because these copolymers have much lower initial crystallinity and thicker amorphous region. The amorphous region can keep the high mobility even after the formation of some tiny crystals in it, as evidenced by the slight increase of glass transition temperature, and the secondary crystallization cannot lead to significant mechanical effects.

Conclusions

The embrittlement of P(3HB-*co*-3HH) with 3HH fractions ranging from 5 to 18 mol % were studied, and the mechanism behind this phenomenon was investigated. It was found that the high initial crystallinity and the narrower interlamellar amorphous region are the key factors that made the secondary crystallization leads to drastic mechanical effects on the copolymer with 3HH fraction lower than 10 mol %. Because of the lower initial crystallinity and the thicker interlamellar amorphous region, the secondary crystallization have less effect on the mechanical properties of the P(3HB-*co*-3HH) copolymers with 3HH fractions higher than 10 mol %. This emphasizes the importance of solid-state structures including the crystallinity and the morphological structures on the mechanical properties and aging phenomenon of polymers.

References and Notes

(1) Müller, H. M.; Seebach, D. *Angew. Chem.* **1993**, *105*, 483.
(2) Doi, Y. In *Microbial Polyesters*; VCH Publishers: New York, 1990.
(3) Lemoigne, M. *Bull. Soc. Chim. Biol.* **1926**, *8*, 770.
(4) Steinbüchel, A.; Füchtenbusch, B. *Trends Biol. Technol.* **1998**, *16*, 419.
(5) Anderson, A. J.; Dawes, E. A. *Microbiol. Rev.* **1990**, *54*, 450.
(6) Barham, P. J.; Keller, A. J. *Polym. Sci. Polym. Phys. Ed.* **1986**, *24*, 69.
(7) Grassie, N.; Murray, E. J.; Holmes, P. A. *Polym. Degrad. Stab.* **1984**, *6*, 95.
(8) Yoshie, N.; Menju, H.; Sato, H.; Inoue, Y. *Macromolecules* **1995**, *28*, 6516.
(9) Byrom, D. *Trends Biotechnol.* **1987**, *5*, 246.
(10) Bluhm, T. L.; Hamer, G. K.; Marchessault, R. H.; Eyfe, C. A.; Veregin, R. P. *Macromolecules* **1986**, *19*, 2871.
(11) Allegra, G.; Bassi, I. W. *Adv. Polym. Sci.* **1969**, *6*, 549.
(12) Scandola, M.; Eccorulli, G.; Pizzoli, M.; Gazzano, M. *Macromolecules* **1992**, *25*, 1405.
(13) Liebergesell, M.; Mayer, F.; Steinbüchel, A. *Appl. Microbiol. Biotechnol.* **1993**, *40*, 292.
(14) Doi, Y.; Kitamura, S.; Abe, H. *Macromolecules* **1995**, *28*, 4822.
(15) Asrar, J.; Velentin, H. E.; Berger, P. A.; Tran, M.; Padgette, S. R.; Garbow, J. R. *Biomacromolecules* **2002**, *3*, 1006.
(16) Feng, L.; Watanabe, T.; Wang, Y.; Kichise, T.; Fukuchi, T.; Chen, G. Q.; Doi, Y.; Inoue, Y. *Biomacromolecules*, **2002**, *3*, 1071.
(17) de Koning, G. J. M.; Lemstra, P. J. *Polymer* **1993**, *34*, 4089.
(18) de Koning, G. J. M.; Scheeren, A. H. C.; Lemstra, P. J.; Peeters, M.; Reynaers, H. *Polymer* **1994**, *35*, 4598.
(19) El-Hadi, A.; Schnabel, R.; Straube, E.; Muller, G.; Henning, S. *Polym. Test.* **2002**, *21*, 665.
(20) Vonk, C. G. J. *Appl. Crystallogr.* **1973**, *6*, 148.
(21) Abe, H.; Doi, Y.; Aoki, H.; Akehata, T. *Macromolecules* **1998**, *31*, 1791.
(22) Tian, G.; Wu, Q.; Sun, S.; Noda, I.; Chen, G. Q. *J. Polym. Sci., Part B: Polym. Phys.* **2002**, *40*, 649.

MA070418I